UDK 669.131.6:661.666.2
Original scientific article/Izvirni znanstveni članek

ISSN 1580-2949
MTAEC9, 56(2)217(2022)

A MODIFIED TEST FOR DETERMINING THE FLUIDITY OF DUCTILE CAST IRON

MODIFICIRAN TEST ZA DOLOČEVANJE LIVNOSTI SIVE LITINE S KROGLASTIM GRAFITOM

Matic Žbontar*, Mitja Petrič, Primož Mrvar

Department of Materials and Metallurgy, Faculty of Natural Sciences and Engineering, University of Ljubljana, 1000 Ljubljana, Slovenia

Prejem rokopisa – received: 2022-01-11; sprejem za objavo – accepted for publication: 2022-02-24

doi:10.17222/mit.2022.367

The aim of this experimental work was to design a modified test with which it will be possible to determine the fluidity of ductile cast iron. First, we planned the conceptual verification of the designed experiment, which was done by numerical simulations of the casting processes, followed by rapid mould fabrication using 3D printing. A measurement cell was placed in the mould cavity of the experimental chamber for further investigation of the cooling and solidification during casting. From the matrix of data obtained with the experiment, we defined the fluidity of the ductile iron EN-GJS-500-7. Also, we analysed the mechanical properties of the studied alloy, the microstructure, the chemical composition, and the results of the thermal analysis. In accordance with the expectations and theory from the literature, the fluidity in the experimental sample cast at a higher temperature was better than that cast at a lower temperature. Because of the faster cooling rate at the end of the channel of the experimental casting, the microstructure is fine, moreover, we obtain white solidification, ledeburite in the microstructure of the samples etched with Nital. At lower cooling rates, fewer graphite nodules appear in the microstructure, which are larger, and the portion of ferrite is greater.

Keywords: spheroidal graphite cast iron, fluidity, microstructure, simple thermal analysis

Cilj eksperimentalnega dela je bil zasnovati modificiran preskus, s katerim bo mogoče določiti livnost sive litine s kroglastim grafitom. Najprej smo načrtovali konceptualno preverjanje načrtovanega poskusa, ki smo ga izvedli z numeričnimi simulacijami postopkov litja, čemur je sledila hitra izdelava kalupov s 3D tiskanjem. Za nadaljnje raziskave ohlajanja in strjevanja med litjem je bila v votlino kalupa eksperimentalne komore nameščena merilna celica. Na podlagi podatkov, pridobljenih z eksperimentom, smo opredelili tekočnost duktilne litine EN -GJS-500-7, nadalje smo analizirali mehanske lastnosti preučevane zlitine, mikrostrukturo, kemijsko sestavo in rezultate termične analize. V skladu s pričakovanji in teorijo iz literature je bila tekočnost poskusnega vzorca, ulitega pri višji temperaturi, boljša od vzorca, ulitega pri nižji temperaturi. Zaradi hitrejšega ohlajanja na koncu kanala poskusnega litja je mikrostruktura drobna, poleg tega v mikrostrukturi vzorcev, jedkanih z Nitalom, dobimo belo strjevanje - ledeburit. Pri nižjih hitrostih ohlajanja se v mikrostrukturi pojavi manj grafitnih nodul, ki so večje, večji pa je tudi delež ferita.

Ključne besede: siva litina s kroglastim grafitom, livnost, mikrostruktura, enostavna termična analiza

1 INTRODUCTION

Cast iron is known as nature's gift to foundrymen because it melts at easily attainable temperatures, has low energy consumption, flows like water, is tough enough for many engineering applications, and is relatively insensitive to a poor casting technique. The commercial use of simple grey cast iron was one of the key factors for the start of the industrial revolution, but the range of other ferrous alloys is also very wide.[1]

In foundry terminology, fluidity is the distance to which the alloy, cast at a given temperature, flows through the runner of the test mould before it is stopped by the solidification process. In metallurgy, fluidity is the ability to fill thin walls or sections. Many papers emphasize the misinterpretation of fluidity with viscosity, which is strongly disagreed with by metallurgists, as there are many more factors that affect the fluidity than just the viscosity. Fluidity expertise is important for foundrymen as well as theorists and researchers. Theorists try to find an accurate model for determining the fluidity, but there are so many factors to consider that the problem has not yet been fully solved. Researchers find fluidity important because there is still no standard method for determining it that returns tangible results. Problems and deviations occur with many known methods, and the repeatability of the experiments is low.[2–4]

One of the most important parameters for determining the melt flow in the runner and cavity is fluidity, which depends on the type of alloy, the solidification morphology, superheat, viscosity, surface tension, oxidation of the melt surface, dissolved gases and inclusions, mould properties, metallostatic pressure and many more. Fluidity is an important characteristic as it limits the wall thickness of a casting that can be completely filled. Research into fluidity is particularly important for the automotive and aerospace industries in order to produce thinner, lighter, and cheaper parts. It is associated with problems such as cavity filling, feeding, porosity, hot tearing and macrosegregation.[5,6]

*Corresponding author's e-mail:
matic.zbontar@ntf.uni-lj.si

Fluidity is highly dependent on the thermal modulus of a casting's sections, which influences the cooling and solidification. It originates from the simpler geometrical modulus, which is defined as the ratio volume/cooling area, but also takes into account different foundry materials used and their thermal behaviours.

Traditionally, fluidity measurements are made using spiral channel moulds, which can be disposable (sand) or permanent. The use of the spiral mould is logical as the mould takes up as little space as possible and therefore the experimental mould is as small as possible. The entire test channel is in the same plane when determining fluidity, as the melt flow can be influenced by the different channel heights in the mould. In research practice, many different variants of spiral test moulds have already been verified.[3,6–9]

Strip tests to determine the fluidity are both traditional and still widely used,[3,10–12] but the question arises as to the effect of one channel being closer to the down sprue than the other. The dilemma is avoided by the design shape used in papers,[8,9,13,14] but the latter two may be the most size efficient as they use spiral shapes for the channels.

The fluidity measurements are presented as a percentage fill or length in different cross-sectional channels of a test mould, as described in the papers,[3,8–10] has proven to be a useful and accurate practise applicable to different types of castings (thin- and thick-walled). In the present study, the aim was to design a different test mould to show the fluidity as a function of flow length in three differently shaped channels of the same mould. For this purpose, two experimental moulds were first developed and tested in a ductile-iron foundry. These are presented below.

2 EXPERIMENTAL PART

For the fluidity determination, two moulds were 3D printed using silica casting sand and furan binder. The goal was to measure the temperature as accurately as possible during cooling and solidification in the casting, so a thermocouple was included in the casting cavity. For convenience, ease of use and reproducibility of the experiment, it was decided to use a Quik-Cup probe (with a type-K thermoelement NiCr-Ni), used for a Simple Thermal Analysis, at the bottom of the cell. To avoid the melt flowing directly onto the quartz protection tube of the thermocouple, a core with an opening outside the centre of the funnel was designed. This core confines the measuring cell to the remaining casting cavity of the experimental mould. The top of the casting, or the top of the mould, was designed to pour the melt into a basin from which it flows more uniformly through a filtering system that subsides the flow of the melt (reducing turbulence and removing non-metallic inclusions) before it begins to fill the casting cavity. During the model's development, corrections were also made to the geometries of the individual variants in accordance with the casting-process calculations. Based on the results, the final dimensions of the channel cross-sections and all the other dimensions of the casting-system elements were selected. The casting-process calculations were performed in ProCAST (ESI Group, Paris, France), a software based on the finite-element method (FEM). The final geometry consisted of a pouring basin, a down sprue, a biscuit-shaped distribution chamber with three spirals of triangular, semicircular, and trapezoidal shape extending from it, and a Quik-cup area below. The three cross-sectional shapes were selected to ensure easy moulding (parting line on the top of all three channels). The shapes were designed to have approximately the same cross-sectional area with which the volume flow through is the same. On the other hand, the channels have different perimeters and therefore geometrical and thermal moduli, which influences greatly the cooling and solidification. Other gating-system elements were also selected according to the moulding pattern practices in the foundry. With that the design is moulding-pattern ready. The final

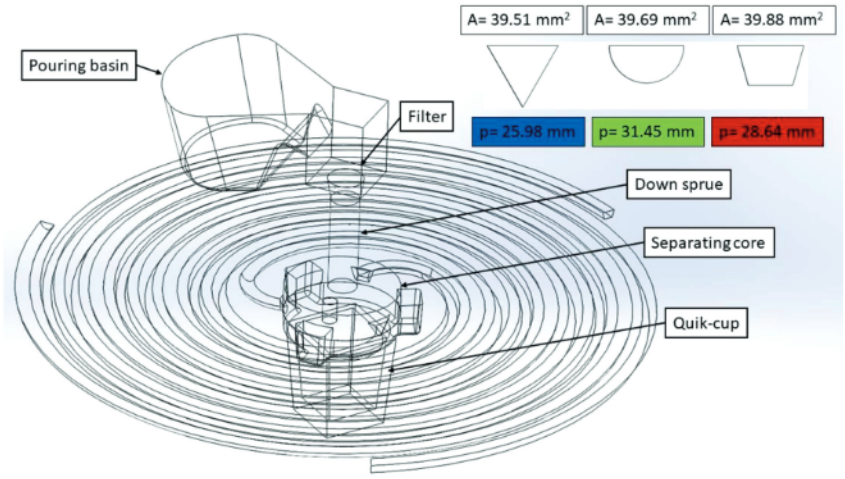

Figure 1: Illustration of triangular, semi-circular, and trapezoidal channel shape with actual cross-sectional areas and perimeters alongside a schematic representation of the experimental mould cavity

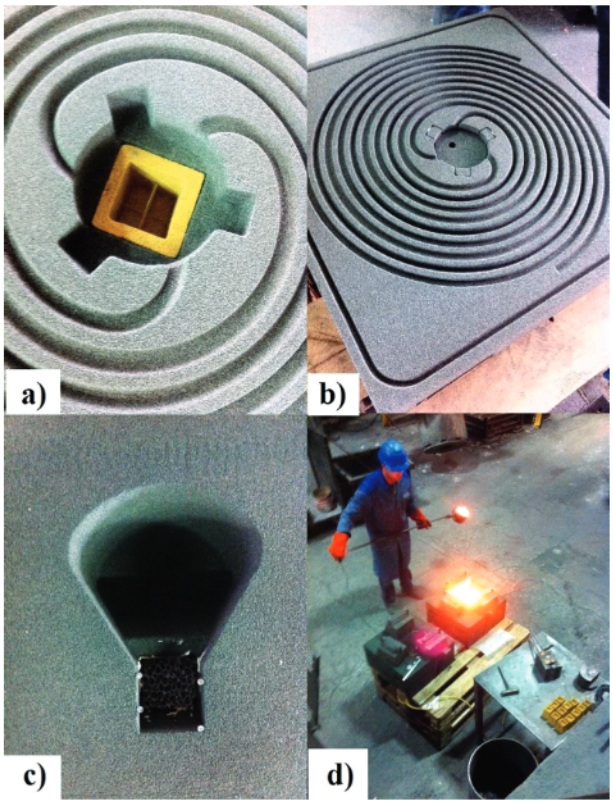

Figure 2: Mould-assembly sequences and manual gravity casting

cross-sections of the channels are shown in **Figure 1** with the actual area (*A*) and perimeter (*p*).

The Quik-cup thermal analysis cell was placed in the mould drag, a separation core was inserted to confine the cavity with the measuring cell, and then the mould was assembled. A ceramic filter was inserted into the upper side of the cope above the down sprue, and the Quik-cup was connected to the ATAS metstar computer system (Novacast, Ronneby, Sweden). The cast iron used for the two test moulds was the same as used in the foundry production line at the time of the experiment, the base metal was a cupola melt combination of scrap steel, pig iron, flux additions, and coke and later the treatment consisted of a sandwich procedure with FeSiMg for the nodulation. Experimental moulds were cast at different temperatures, which was achieved with the difference in pouring time of the mould (same alloy). There were no other process variables. **Figure 2** shows the steps in the experimental:

a) Quik-cup measuring cell inserted in the mould drag,
b) drag of the mould with separating core placed over the Quik-cup already placed,
c) upper side mould cope where pouring basin is seen and ceramic filter is placed on top of down sprue,
d) experimental mould right after the test.

Manual gravity casting of SGI EN-GJS-500-7 at two different casting temperatures (accurate measurements of the two were determined by Simple Thermal Analysis) was performed using 8-kg crucibles. Immediately after the casting of each experimental mould, a Y-sample and a chemical composition sample were cast. Tensile tests were performed on the INSTRON 5985 (Instron, Norwood, Massachusetts, USA) and data were analysed using Bluehill software. Chemical analysis was performed on thin, white solidified plates on the ARL Metal Analyzer IRON + STEEL (Thermo Fischer Scientific, Waltham, Massachusetts, USA). The samples for metallography were prepared by sanding and polishing. The microstructure of the samples was first recorded in the polished state, to observe and determine the pearlite and ferrite contents, they were etched in 2 % Nital before the microscopy. An Olympus BX 61 optical microscope with a DP70 video camera (Olympus Europa SE & Co. KG, Hamburg, Germany) and analySIS 5.0 software were used to observe the microstructure of the polished and etched samples. The analySIS 5.0 software was used to determine the percentage, shape, size and distribution of graphite and the portion of ferrite and pearlite in the matrix of the investigated SGI according to the EN ISO 945 standard.

3 RESULTS AND DISCUSSION

The simulation results showed that the design of the experimental mould is suitable, and the length of the spirals is long enough to determine the fluidity of the melt. The virtual experiment showed that the melt flowed approximately the same path in triangular and trapezoidal channels. The flow length in the semicircular channel was much shorter. The melt filled 91.3 % of the entire experimental casting cavity before it solidified.

The chemical composition of the ductile iron used for experimental testing and a determination of the fluidity is shown in **Table 1**. The chemical composition was not specifically controlled for the experiments, but simply used as it existed in the foundry at the time of the experiment.

The fluidity of the two test moulds, measured for each individual channel using a string and tape measure, is shown in **Figure 3**.

Although there were no significant differences in flowability between the differently shaped channels as expected, we can still draw some conclusions. It is known that the casting temperature has a direct influence on the fluidity, which is evident from the results. For both casting temperatures, the longest flowability was

Table 1: Chemical composition of investigated SGI 500-7 used for fluidity experiment

element	C	Si	Mn	S	Cr	Cu	P	Mg	Ni	Mo	V	Ti	Sn	Bi
w/%	3.54	2.66	0.23	0.01	0.03	0.03	0.03	0.04	0.02	< 0.01	< 0,01	0.01	0.03	< 0.01

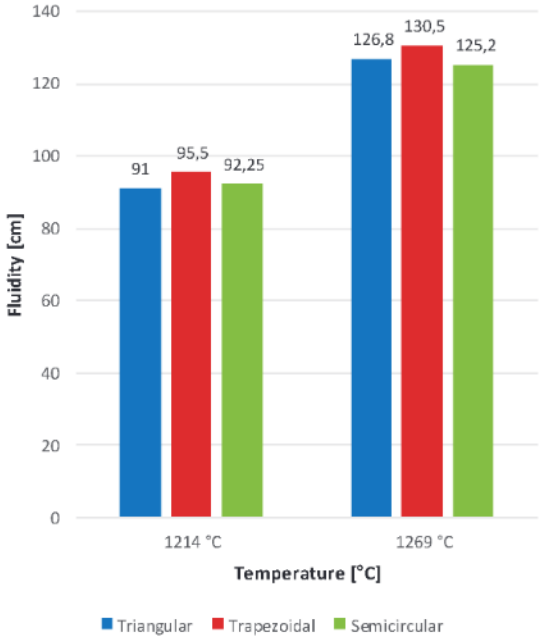

Figure 3: Fluidity of investigated SGI 500-7 expressed in centimetres as a function of casting temperature for differently shaped spiral channels

obtained for the trapezoidal-shaped channel. The trapezoidal channel shows the best fluidity results at both casting temperatures, which can be easily related to the thermal modulus of the channels and thus the cooling rates. The thermal modulus for the triangular, trapezoidal, and semicircular channels (calculated using ProCast simulation) are (0.193, 0.195, and 0.2) cm respectively.

The relationship between the thermal modulus and the fluidity of each channel cannot be used to compare the results of the triangular and semicircular channels, which could be due to a smaller difference in the thermal modulus.

The thermal analysis diagrams showing the cooling curves, its derivatives and recorded characteristic temperature points are shown in **Figure 4**. The black curve presents the cooling, red the 1st derivate and violet the 2nd one. The horizontal lines T_{eW} and T_{eG} indicate a theoretical temperature at which white, under metastable conditions (T_{eW}) and grey (T_{eG}) solidification take place for the analysed material (SGI 500-7) and are calculated according to the silicon content from the material database. The areas marked in different colours under the cooling curve are as follows: green is for the liquid state, yellow (which is so small that is hardly visible, as usual for ductile irons) for primary austenite growth, orange represents the first part of the eutectic reaction during which graphite and austenite are precipitated between temperatures T_{low} and T_{high} and red represents the second part of eutectic solidification between temperatures T_{high} and T_S (solidus temperature). The grey area is where the sample is already in the solid state. T_L indicates the liquidus temperature and the start of precipitation. The lowest eutectic temperature (T_{Elow}) is the minimal point from which the temperature is increasing and T_{Ehigh} is the highest eutectic temperature, the maximum temperature after the increase in temperature. For the eutectic composition T_L and T_{Elow} are the same. If T_{Elow} is too low, that would indicate that the nucleation is not efficient and the risk for primary cementite precipitation increases.

Graphite factor 1 (GRF 1) is an indicator that reflects how much eutectic is precipitated during the second phase of the eutectic, i.e., between T_{Ehigh} and T_S. Graphite factor 2 (GRF 2) uses heat conductivity to estimate the amount and type of graphite at the end of freezing. ACEL is the active carbon equivalent and is calculated from the contents of C, Si and P (Equation (1)):

$$\text{ACEL} = \text{C} + \text{Si}/4 + \text{P}/2 \quad (1)$$

Optimal value for ACEL in ductile irons is 4.3 (eutectic).

From the melt-quality results tables obtained with the ATAS metstar system, high values of recalescence R (difference between T_{low} and T_{high}) are evident, indicating that a relatively large amount of carbon precipitates as graphite, leading to rapid volume expansion at the beginning of the solidification, such that not much carbon remains for precipitation and shrinkage compensation at the end of solidification, making this a relatively poor-quality result. T_{Elow} for the casting temperatures 1269 °C and 1214 °C are 1135 °C and 1133.2 °C, respectfively.

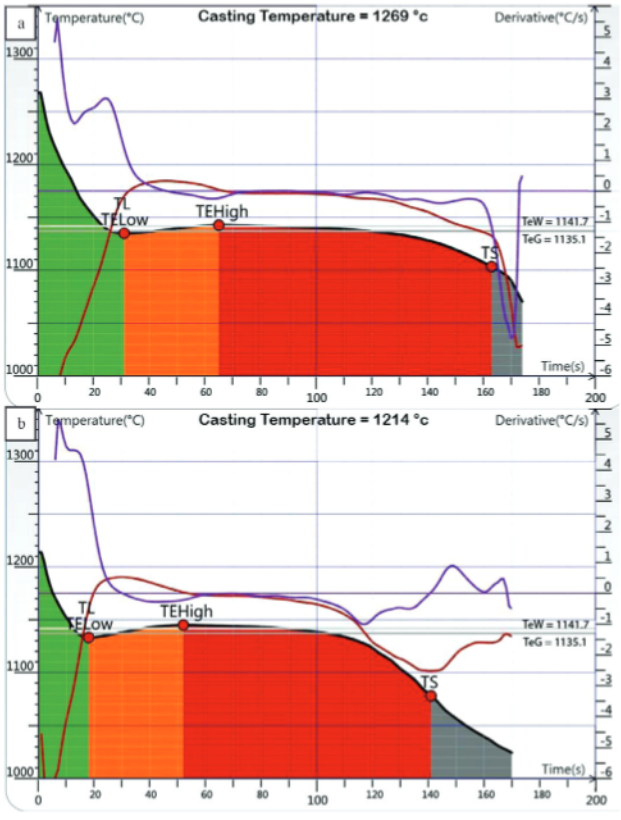

Figure 4: Thermal analysis diagram for experimental moulds cast at: a) higher temperature (1269 °C), b) lower temperature (1214 °C)

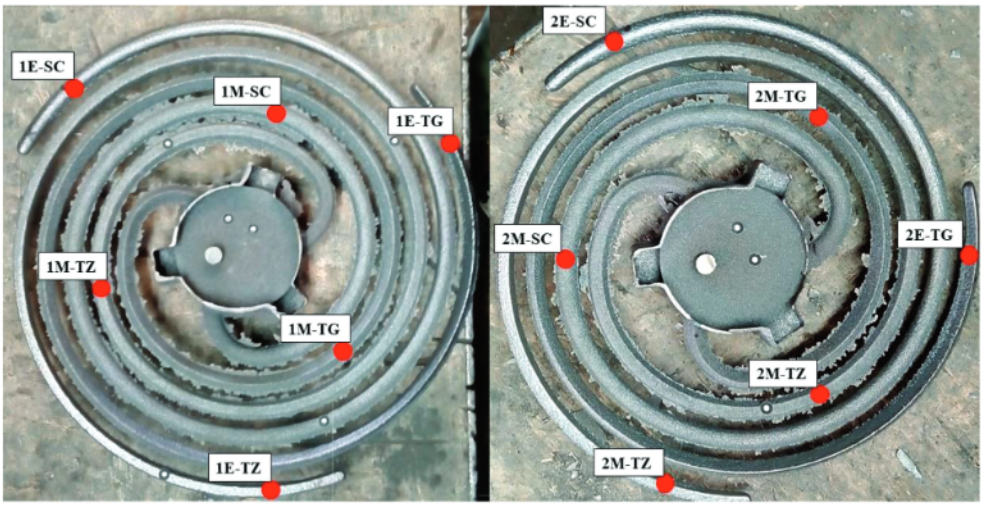

Figure 6: Sample sites for metallography of experimental moulds cast at higher (left) and lower (right) casting temperatures

Relatively low T_{Elow} values observed in both results imply a low nucleation potential, risk of premature solidification in thin-walled sections, risk of undercooled graphite structures and increased solidification shrinkage. The GRF1 values are within the recommended limits, while the GRF2 values are much too high, which may indicate a lack of spheroidal graphite and again the tendency for microshrinkage porosity. The ACEL values are for casting temperatures 1269 °C and 1214 °C, 4.35 and 4.36 respectfully. If ACEL exceeds a value of 4.3, which applies to the melt-quality results of a test casting at lower temperature, there is a possibility of primary graphite crystallization (hypereutectic solidification), resulting in a lower content of the eutectic (γ + G). The consequence may again be an increased shrinkage during solidification. Nevertheless, the results of the two thermal analyses (both at higher and lower casting temperatures) show no difference between the liquidus temperature T_L and the lower eutectic temperature T_{Elow}, indicating a eutectic or near-eutectic composition. Therefore, the values of ACEL, T_L and T_{ELow} are also consistent with the chemical composition of the analysed alloy based on the Fe-C-Si phase diagram. Another indicator that is outside the recommended range only for the experimental mould cast at lower temperatures is T_S (solidus temperature) with a value of 1077.9 °C, which deviates from the lower limit, implying an increased risk for the formation of ledeburite in the final phase of solidification.

Stress-strain curves for the investigated alloy cast in the first and second experimental moulds were obtained. The tensile strength (R_m) of the specimen cast at 1269 °C was 604.4 MPa, that of the second (cast at 1214 °C) 609.4 MPa, and the yield strength ($R_{p0.2}$) was 353.8 MPa (1269 °C) and 360.6 MPa (1214 °C), respectively. The tensile elongation during braking was 13.3 % (1269 °C) and 12.5 % (1214 °C), respectively. The obtained mechanical properties of the materials exceed the required values for ductile iron EN-GJS-500-7, which should be at least 500 MPa for tensile strength, 320 MPa for yield strength and 7 % for elongation.

The samples for microstructural analysis of the experimental moulds cast at both casting temperatures were taken from the areas indicated in **Figure 6**. The range markings are as follows:

- 1 represents the first experimental mould,
- 2 represents the second experimental mould,
- E and M denotes sampling location (E at the end of the spiral channel and M at about the middle of the flow length),
- SC, TG, TZ denote the shape of the channel section (SC- semicircle, TG- triangle, TZ- trapezoid).

The matrix is mostly pearlitic with a bulls eye, the sample from the Y-shaped specimens for mechanical testing showed that the average percentage area of pearlite is 71.8 %, which is consistent with the results of the mechanical testing (average R_m = 607 MPa, average elongation A = 12.9 %).

It is surprising that the strain during braking was relatively high according to the determined ferrite content in the matrix. Typical polished sample microstructure of analysed SGI is shown on **Figure 7a** to **7d** present different matrix of our samples. Crucial parts and microstructural constituents are shown on **Figure 8**.

The samples from the first experimental mould cast at 1269 °C, taken at the end of the spiral, have slightly smaller graphite nodules than those taken in the middle of the spiral channels, while the etched samples have a high portion of carbides from ledeburite. The etched samples from the middle of the channels show a higher portion of ferrite surrounding the graphite nodules, while no carbides from the ledeburite are observed (**Figure 7a**). The results are directly correlated with the higher cooling rates at the end of the spirals. Also, the samples from the mould cast at 1214 °C show that the samples taken from the end of the channels have smaller graphite nodules with very little ferrite surrounding

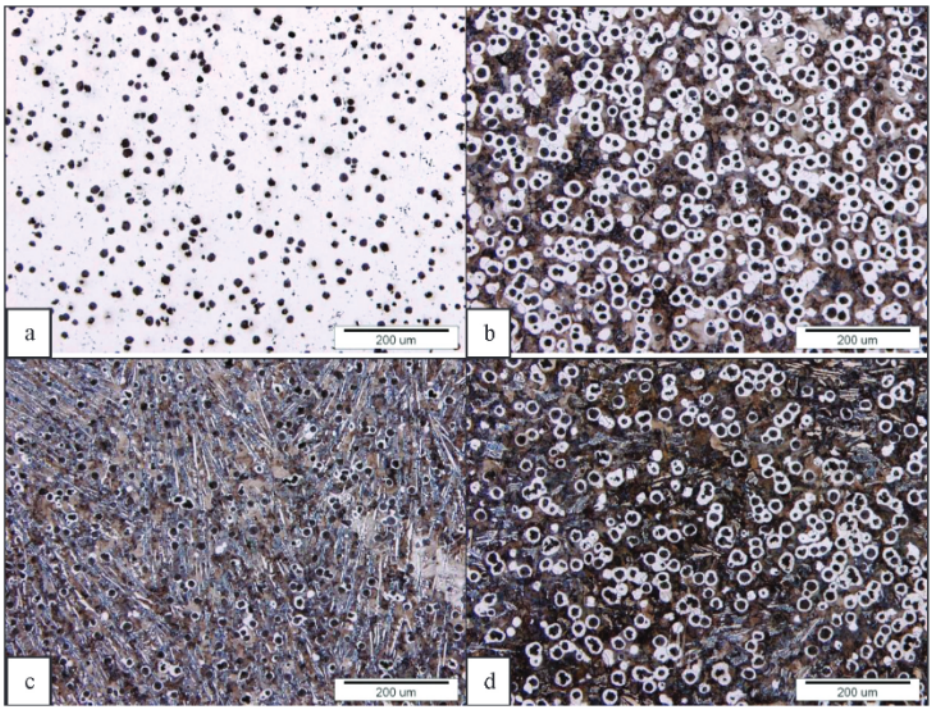

Figure 7: Microstructure of analysed SGI: a) polished sample 1M-TG, b) etched sample 1M-TG, c) etched sample 2E-TG, d) etched sample 2M-SC

them, and as for the etched samples, carbides (in addition to samples from the end of the channels, see **Figure 7c**) are also found in the samples taken from the middle of the channels (**Figure 7d**).

Quantitative results for marked sites from **Figure 6** are shown in **Table 2.** The values for the (graphite) shape, which are given in the second column for the individual sample, are schematically presented in **Figure 9**. Nodularity, presented in the third column, is a value that tells us how rounded the graphite nodules are (1 being a perfect circle). Area fraction in percent shows us how much of the analysed area (0.585 mm^2) covers graphite and the number of nodules is the number of graphite particles on that same area.

A higher percentage of nodules is associated with higher cooling rates. This is very clear from **Table 2** for the samples of the first experimental mould, but cannot be clearly related to the results of the second experimental mould, which was cast at 1214 °C. The number of larger nodules was higher from the samples taken in the middle of the cast length from both experimental moulds and the number of smaller nodules is lower, which is only true for the first experimental mould. The majority of the determined graphite particles from the analysed microstructures have size 7 and shape V, i.e., nodular, but

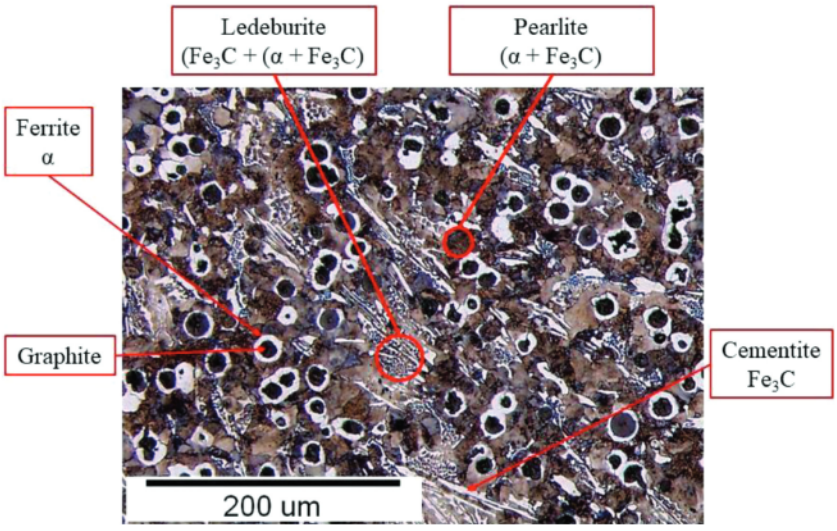

Figure 8: Zoomed in microstructure of sample 2E-TZ with marked microstructural constituents

Table 2: Results of microstructural analysis on graphite

Sample	Shape	Nodularity	Area fraction (%)	No. nodules	No. Nodules size 6 (< 60 µm)	No. Nodules size 7 (< 30 µm)	No. Nodules size 8 (< 15 µm)
1E-SC	V	0.537	6.483	1779	28	1283	468
1E-TG	V	0.534	5.768	1750	18	1186	546
1E-TZ	V	0.532	6.003	1765	23	1220	522
1M-SC	V	0.537	8.824	1706	122	1299	285
1M-TG	V	0.523	7.857	1751	89	1270	392
1M-TZ	V.III (25 %)	0.502	6.464	1546	93	1125	328
2E-SC	V	0.513	6.517	1572	69	1145	358
2E-TG	V	0.506	5.481	1522	52	1022	448
2E-TZ	V.III (25 %)	0.490	5.497	1580	62	1052	466
2M-SC	V.III (25 %)	0.506	6.305	1754	67	1144	543
2M-TG	V	0.519	7.770	1602	116	1182	304
2M-TZ	V.III (30 %)	0.486	5.463	1583	67	1047	469

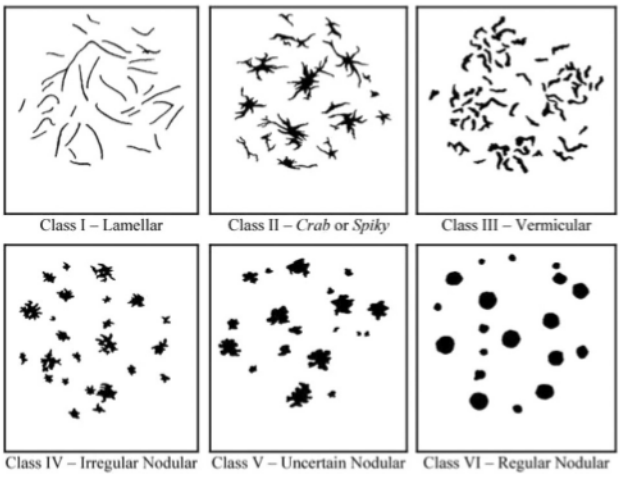

Figure 9: Schematic representation of different graphite shapes which could be found in cast irons[15]

there is a tendency for some particles exhibiting shape III, which is more frequent for the microstructures of the second experimental mould. The phenomenon of inconsistent results from the experimental mould number two, which was cast at a lower 1214 °C, could be related to the fact that the casting temperature was too low and therefore the solidification and structure formation of the ductile iron was not optimal. The other reason could also be the fading effect of Mg. The areas of the casting at the end of the flow length of the spirals have the highest cooling rate, which evidently exceeds the critical cooling rate at which full grey solidification is still possible. Therefore, at the sampling points 1E-SC, 1E-TG, 1E-TZ and 2E-SC, 2E-TG, 2E-TZ, a significant part of the microstructure consists of primary austenite crystals undergoing eutectoid transformation to ferrite and graphite and/or to pearlite, graphite eutectic ($\gamma + G$) and metastable eutectic ledeburite ($\gamma + Fe_3C$). Primary austenite crystals and both austenites from the eutectics transformed to ferrite and graphite and mainly to pearlite. To clarify, primary austenite is present in the microstructure due to higher cooling rates in thin-walled channels and metastable solidification even though our investigated SGI had eutectic or slightly hypereutectic composition according to thermal analysis results. It was found that there were no significant changes in the microstructure between samples with different channel cross sections taken at the same length, but that there were visible differences at a microscope magnification of 200 × when comparing samples with different flow lengths.

4 CONCLUSIONS

Using modern methods of modelling, design, and calculation of the casting processes, preliminary validation of an experimental cell for the determination of fluidity in a virtual environment was performed.

Prototype experimental moulds for the determination of fluidity were successfully produced using 3D printing of sand mixture, which were additionally instrumented by an in-situ temperature measurement (Simple Thermal Analysis).

Experimental tests on two cells were successfully performed under industrial conditions.

The temperature of 1214 °C inside the experimental mould is relatively low and causes irregularities in the microstructure. To perform a precise microstructure analysis and to clearly link the results to the results of the fluidity measurements is therefore not possible.

The newly developed test enables accurate recordings of the experimental temperatures of the melt under investigation.

The measured fluidity results were accurately determined for each channel geometry and are relatively consistent in terms of comparative reproducibility when differences in the casting temperature are considered.

The fluidity, expressed in terms of the total flow length of the experimental mould, was 278.75 cm and 382.50 cm for 1214 °C and 1269 °C, respectively. It was found that the trapezoidal channel has the best fluidity at a constant channel cross-section, while the triangular and

semicircular channels have poorer fluidity. Therefore, the fluidity in the trapezoidal channel of the studied SGI cast iron, grade 500, is 95.5 cm at 1214°C and 130.5 cm at 1269 °C. This result is also correlated with the thermal modulus and hence the cooling rate and was somewhat expected in advance. A Larger series of experiments IS still required to further determine the applicability and accuracy of the proposed test. The proposed test is designed to allow pattern moulding, which is vital for simple and economical large-scale testing.

5 REFERENCES

[1] J. Campbell, Complete Casting Handbook: Metal Casting Processes, Metallurgy, Techniques and Design. Second Edition, Elsevier, 2015

[2] B. Dewhirst, Castability Control in Metal Casting via Fluidity Measures: Application of Error Analysis to Variations in Fluidity Testing, Worchester: Faculty of the Worcester polytechnic institute, 2008

[3] J. Campbell, R. A. Harding, The Fluidity of molten metals. Birmingham: The University of Birmingham, 1994

[4] A. Aran, Manufacturing properties of engineering materials: Lecture notes. ITU, Department of Mechanical Engineering, 2007

[5] Trbižan, M. Livarstvo: internal script. Ljubljana. Faculty of natural sciences and engineering, Department of materials and metallurgy, 1994

[6] M. Di Sabatino, F. Syvertsen, L. Arnberg, A. Nordmark, An improved method for fluidity measurement by gravity casting of spirals in sand moulds. International Journal of Cast Metals Research, 18 (**2005**), 59–62, doi:10.1179/136404605225022865

[7] M. Di Sabatino, S. Shankar, D. Apelian, L. Arnberg, Influence of temperature and alloying elements on fluidity of Al-Si alloys, TMS 2005, Shape Casting: The John Campbell Symposium, 2005, 193–202

[8] M. Gorny, Castability of ductile iron in thin walled castings, Archives of foundry engineering, 8 (**2008**) 3, 59–6

[9] M. Gorny, Fluidity and Temperature Profile of Ductile Iron in Thin Sections, Journal of Iron and Steel Research, International, 19 (**2012**) 8, 52–59, doi:10.1016/S1006-706X(12)60139-3

[10] M. Çolak, S. Kaya, Investigation of the Effect of Inoculant and Casting Temperature on Fluidity Properties in the Production of Spheroidal Graphite Cast Iron, Trans Indian Inst Met., 74 (**2021**) 2, 205–214, doi:10.1007/s12666-020-02159-5

[11] A. H. Fazeli, H. Saghafian, S. M. A. Boutorabi, J. Campbell, The Fluidity of Aluminium Ductile Irons, Inter Metalcast, 16 (**2021**), 143–152, doi:10.1007/s40962-021-00581-z

[12] S. Slamet Suyitno, I. Kusumaningtyas, Effect of composition and pouring temperature of Cu (20-24) wt.% Sn by sand casting on fluidity and Mechanical Properties. Journal of Mechanical Engineering and Science, 13 (**2019**) 4, 6022–6035, doi:10.4108/eai.24-10-2018.2280525

[13] S. R. Pulivarti, A. K. Birru, Effect of Mould Coatings and Pouring Temperature on the Fluidity of Different Thin Cross-Sections of A206 Alloy by Sand Casting, Trans Indian Inst Met, 71 (**2018**), 1735–1745, doi:10.1007/s12666-018-1311-2

[14] M. Borouni, B. Niroumand, M. H. Fathi, Effect of a nano-ceramic mold coating on the fluidity length of thin-wall castings in Al4-1 alloy gravity sand casting, Mater. Technol., 48 (**2014**), 473–477

[15] O. Gomes, S. Paciornik, Automatic classification of graphite in cast iron, Microscopy and Microanalysis, 11 (**2005**) 4, 363–371, doi:10.1017/S1431927605050415